



In-situ synthesis, thermal and mechanical properties of biobased poly(ethylene 2,5-furandicarboxylate)/montmorillonite (PEF/MMT) nanocomposites

Hongzhou Xie^a, Hongxu Meng^a, Linbo Wu^{a,*}, Bo-Geng Li^a, Philippe Dubois^{b,*}

^a State Key Laboratory of Chemical Engineering at ZJU, Key Laboratory of Biomass Chemical Engineering of Ministry of Education, College of Chemical and Biological Engineering, Zhejiang University, Hangzhou 310027, China

^b Laboratory of Polymeric and Composite Materials (LPCM), Center of Innovation and Research in Materials and Polymers (CIRMAP), University of Mons, Mons 7000, Belgium

ARTICLE INFO

Keywords:

Bio-based polyester
Poly(ethylene 2,5-furandicarboxylate)
Polymer nanocomposites
Crystallization
Polymer modification
Montmorillonite

ABSTRACT

Poly(ethylene 2,5-furandicarboxylate) (PEF) is an emerging biobased polyester well-known for high gas barrier properties as well as high tensile modulus and strength, but PEF modification is still desired to improve its crystallization rate, toughness and even strength. In this study, PEF/Montmorillonite (MMT) nanocomposites were in-situ synthesized via melt polycondensation of dimethyl furandicarboxylate and ethylene glycol in the presence of a commercially available organically modified montmorillonite (OMMT), i.e., DK2, a montmorillonite clay modified with octadecyl hydroxyethyl dimethyl ammonium. The structure of nanocomposites was characterized by ATR-FTIR, ¹H NMR, WAXD and TEM, and their thermal and mechanical properties were assessed with DSC, TGA and tensile test. The OMMT was grafted with PEF chains and therefore exfoliated, at least partially, in the PEF matrix with intrinsic viscosity over 0.7 dL/g. With respect to pristine PEF, the nanocomposites containing 2.5 wt% DK2 showed significantly improved melt crystallization, tensile modulus and strength.

1. Introduction

As a newly emerging bio-based polyester in the last decade, poly(ethylene 2,5-furandicarboxylate) (PEF) is a very promising polymeric material because of its attractive physico-mechanical properties as well as excellent sustainability. Both of its monomers, 2,5-furandicarboxylic acid (FDCA) and ethylene glycol (EG), can be produced from renewable biomass like starch, cellulose or hemicellulose as starting materials [1–4]. Moreover, greenhouse gas emission and non-renewable energy use are predicted to be reduced by 45–55% and 40–50% respectively in PEF production as compared with its petroleum-based counterpart, PET [5]. On the other hand, the more rigid structure of FDCA with respect to terephthalate acid (TPA) endows PEF with higher glass temperature [6], superior stiffness and strength [7,8] and notably higher gas barrier properties than PET [9–11]. Its O₂ and CO₂ permeability are extensively reported to be several times to more than one order of magnitude lower than PET. Because of excellent sustainability and superior material performance, PEF will become a competitive material for applications in eco-packaging as well as engineering materials.

On the other hand, however, PEF is also characterized by slow crystallization [12–14] and brittleness [8,9,12,15,16]. Such shortcomings will hinder its practical processing and applications. To modify PEF, copolymerization [8,9,17–25], blending [26–28] and nanocomposite compounding of PEF [29–35] have been reported in the latest years. Both copolymerization and blending are effective in PEF toughening, but often lead to deterioration of crystallization, stiffness, strength, heat resistance and gas barrier properties. Production of nanocomposites is also a frequently used technology for polymer modification, using various nanofillers having one (layered), two (tube, fibre or whisker) or three (e.g., spherical) dimensions in the order of few nanometers. In comparison with copolymerization and blending, nanocomposite compounding, especially with layered nanofillers, seems to be a more versatile method as it can effectively improve multiple performances of polymers, leading to crystallization promotion [36,37], stiffness/strength enhancement [38,39], gas barrier improvement [36,39,40], and sometimes even toughening of polymer [41,42]. In 2016 and 2017, Martino *et al.* reported morphology and thermal properties of PEF nanocomposites with organically modified

* Corresponding author.

E-mail addresses: wulinbo@zju.edu.cn (L. Wu), philippe.dubois@umons.ac.be (P. Dubois).

montmorillonite (OMMT) or sepiolite prepared by solvent casting and melt blending respectively [30,32]. In these nanocomposites, the presence of intercalated OMMT slightly promoted crystallization of PEF at heating or cooling rate as slow as 2 °C/min. Lotti *et al.* reported that in-situ prepared PEF nanocomposites with multi walled carbon nanotubes (MWCNTs), functionalized MWCNTs or graphene oxide (GO) showed clearly improved melt and cold crystallization with respect to neat PEF as these nanofillers acted as nucleating agents for PEF [34]. Achilias *et al.* also found that TiO₂ nanoparticles clearly accelerated the crystallization of PEF nanocomposite prepared by in-situ melt and solid state polycondensation. [29] However, the research on PEF nanocomposites is still premature. To date, there is no report on mechanical and gas barrier properties of PEF nanocomposites. The crystallization of PEF nanocomposites also needs to be further promoted, especially at fast cooling rate which mimics practical processing condition. For in-situ prepared PEF nanocomposites, higher molecular weight of PEF is also expected.

In this study, PEF/MMT nanocomposites were in-situ prepared via melt polycondensation of dimethyl furandicarboxylate (DMFD) and ethylene glycol (EG) in the presence of a commercially available OMMT, i.e., DK2, an organic montmorillonite modified with octadecyl hydroxyethyl dimethyl ammonium. The nanocomposites were characterized by ATR-FTIR, ¹H NMR, WAXD and TEM, and their thermal and mechanical properties were assessed with DSC, TGA and tensile testing. With respect to pristine PEF, the nanocomposites containing 2.5 wt% DK2 had the same high intrinsic viscosity but showed significantly improved melt crystallization, tensile modulus and strength.

2. Experimental section

2.1. Materials

Dimethyl 2,5-furandicarboxylic acid (DMFD, purity over 99.8%), ethylene glycol (EG, 99%) and stannous oxalate (SnOxa) were purchased from Jiaying Ruiyuan Biotech Co. Ltd (China), Sigma-Aldrich and Aladdin Reagent, respectively. Sodium montmorillonite (Na-MMT) and DK2, an organic montmorillonite modified with octadecyl hydroxyethyl dimethyl ammonium, were purchased from Zhejiang Fenghong New Materials Co. Ltd, China. Ethylene glycol antimony (Sb₂(EG)₃) was kindly provided by Sinopec Yizheng Chemical Fibre Co. Ltd, China. Phenol, 1,1,2,2-tetrachloroethane (TCE) and deuterated trifluoroacetic acid (d₁-TFA) were purchased from Sinopharm. All the chemicals were used as received.

2.2. In-situ synthesis of PEF/MMT nanocomposites

The in-situ synthesis of PEF/MMT nanocomposites was carried out in a three-step process. First, the powdery OMMT, DK2, was dispersed in EG at high speed stirring (1000 r/min) for 12 h and subjected to sonication for 15 min. Then, the resulting dispersion was added, together with DMFD and SnOxa (0.2 mol% based on DMFD), into a 250 mL four-necked round-bottom flask equipped with a mechanical stirrer, N₂ inlet and reflux condenser. The EG/DMFD molar ratio was 2.0. Transesterification reaction was conducted under N₂ atmosphere at 170 °C, 180 °C, 190 °C for 3 * 1 h and then at 200 °C until there was no methanol distilled out. Finally, Sb(EG)₃ (0.1 mol% based on DMFD) was added into the transesterification product, and the temperature was raised to 230 °C and the pressure was reduced slowly to about 110 Pa to start melt polycondensation without the reflux condenser. The reaction lasted for 1 h at 230 °C and 2–2.5 h at 240 °C. The resulting PEF/DK2 nanocomposite was coined as DK2-x in which x was the mass percentage of DK2 feeding based on PEF. It was dried at 70 °C in vacuum for 12 h and stored in a desiccator before characterization.

2.3. Characterization

PEF or its nanocomposites was dissolved in a mixture solvent composed of phenol and 1,1,2,2-tetrachloroethane (3/2, w/w). The resulting solution (5 g/dL) was filtered through a sand core funnel and then used for intrinsic viscosity measurement performed at 25 °C with a semi-automatic viscosity tester (ZONWON IVS300, China) equipped with an Ubbelohde viscometer.

¹H NMR spectra of PEF and its nanocomposites were obtained with Bruker AC-80 (400 M). Deuterated trifluoroacetic acid (d₁-TFA) was used as solvent and tetramethylsilane as internal reference.

ATR-FTIR spectra of PEF and its nanocomposites were recorded with a Nicolet 5700 spectrophotometer (Thermo Fisher Scientific, USA) equipped with a germanium crystal ATR accessory in the wavenumber range of 400–4000 cm⁻¹. Film samples were prepared by hot-pressing molding at 250 °C.

Wide angle X-ray diffraction (WAXD) patterns of PEF and its nanocomposites were recorded on a PANalytical X'Pert X-ray diffraction system (PANalytical Company) with CuKα radiation (1.54 Å), working at 40 kV and 40 mA. Disc specimens were prepared by hot-press molding at 250 °C and then by liquid nitrogen quenching. Thus obtained PEF nanocomposite samples were directly used for WAXD observation, being scanned from 1° to 10° (2θ) with a step size of 0.013° and an acquisition time of 60 s per step. Additionally, the PEF and DK2-2.5 samples were further cold crystallized at 150 °C and 190 °C respectively and then used for WAXD observation, being scanned from 5° to 40° (2θ) with a step size of 0.026° and an acquisition time of 30 s per step.

The dispersion of organic montmorillonite in PEF was observed with JEM-1200EX (JEOL, Japan) transmission electron microscopy (TEM) at an acceleration voltage of 40 kV. Both PEF and its nanocomposites were embedded and microtomed into ultrathin sections.

Thermal transition properties of PEF and its nanocomposites were measured with DSC on a TA-Q200 thermal analyzer (TA Instrument, USA) using a heating-cooling-heating temperature program. The samples were firstly heated from room temperature (RT) to 250 °C at a heating rate of 40 °C/min and kept for 5 min. Then, the cooling/second heating rate of 10 °C/min and isothermal time of 5 min was used in the following steps in the temperature range of 30–250 °C.

Thermal stability of PEF and its nanocomposites was measured with thermogravimetric analysis (TGA) on a TA Q500 analyzer (TA Instrument, USA). All the samples were measured under a nitrogen atmosphere with a heating rate of 10 °C/min from 50 °C to 650 °C.

Tensile properties of PEF and its nanocomposites were measured with a Zwick Roell Z020 (Zwick, Germany) testing machine at room temperature according to ASTM D638. Dumbbell-shaped specimens with 2 mm in thickness and 4 mm in width were prepared by a HAAKE MiniJet injection molding machine. For all the samples, the injection and packing pressure/temperature/time were 1050 Pa/250 °C/15 s and 1020 Pa/100 °C/15 s, respectively. The specimens were conditioned at RT for 48 h before testing. For each sample, at least five specimens were tested. All the specimens were tested at a crosshead speed of 1 mm/min.

3. Results and discussion

3.1. Synthesis and characterization

DK2 was selected as an OMMT to facilitate the in-situ synthesis of PEF nanocomposites. The ATR-FTIR spectrum of Na-MMT and DK2 shown in Fig. 1 evidenced the presence of the organic modifier in the interlayer of DK2. For Na-MMT and DK2, the characteristic peaks at 3621 cm⁻¹ and 1030–400 cm⁻¹ are attributed to the stretching vibration of hydroxy groups on silicate crystal layer and Si-O/Al-O vibrations of silica-alumina layers, respectively. Besides these absorptions of the layered silicates, the characteristic peaks come from the organic modifier, namely, stretching vibrations of CH, symmetrical and

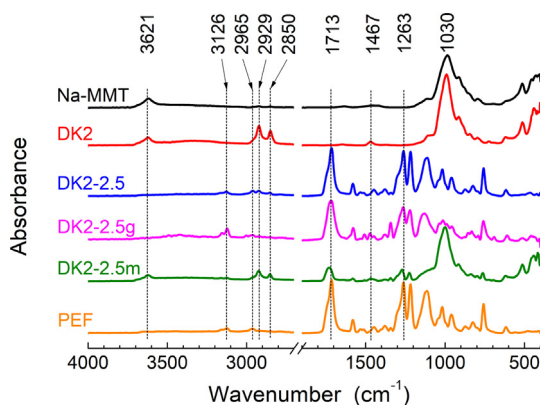


Fig. 1. FTIR spectra of Na-MMT, DK2 (OMMT), DK2-2.5 (PEF/MMT nanocomposite), DK2-2.5g (PEF-grafted OMMT), DK2-2.5m (control) and PEF.

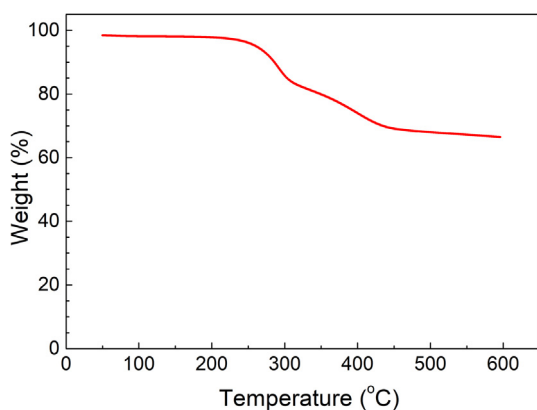


Fig. 2. TGA curve of DK2 under N₂ atmosphere at heating rate of 10 °C/min.

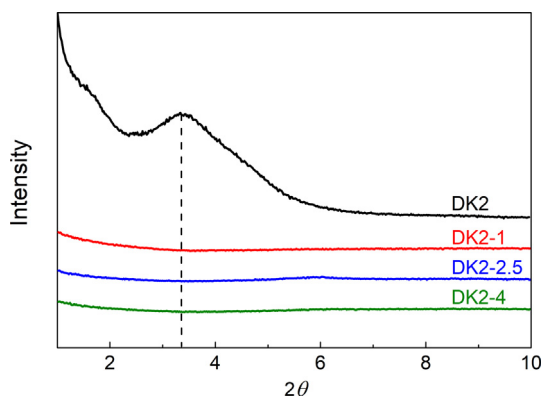


Fig. 3. WAXD patterns of organic montmorillonite (DK2) and PEF nanocomposites quenched from melt.

asymmetrical stretching vibrations of CH₂ appear at 2925 cm⁻¹, 2850 cm⁻¹ and 1467 cm⁻¹, respectively. The result of thermogravimetric analysis indicated the content of the organic modifier in DK2 was about 35 wt% (Fig. 2). Because of the presence of organic modifier with a long alkyl, the WAXD result shown in Fig. 3 indicated that the interlayer distance was broadened from 1.36 nm of Na-MMT to 2.42 nm of DK2.

DK2 was pre-dispersed in EG at high speed stirring (1000 rpm) for 12 h and subjected to sonication for 15 min. Then, DMFD and SnO_x were added to the pre-dispersion and the mixture was heated to start in-situ transesterification. During the pre-polycondensation stage in which the pressure was reduced, clear foaming phenomenon was observed. The formation of foams was ascribed to volatilization of EG along with

the organic modifier which can also be regarded as a surfactant to stabilize the EG bubbles. Severe foaming would result in great loss of reactants. Therefore, the pressure should be carefully and slowly reduced before polycondensation reaction. This process took about 30 min in a 250 mL reactor.

The intrinsic viscosity [η] of PEF reached 0.70 dL/g after melt polycondensation at 240 °C for 2 h. Under the same experimental condition, the presence of 1 wt% DK2 did not affect the chain growth and the resulting nanocomposite DK2-1 had the same [η], but the [η] value was clearly reduced to 0.62 dL/g and 0.59 dL/g at DK2 feeding of 2.5 wt% and 4 wt%, respectively. The results suggest that the presence of higher amount of DK2 hindered the diffusion and removing of EG, the polycondensation byproduct, from the highly viscous reaction system because of the gas barrier effect of the layered silicate. Lower [η] (0.39–0.45 dL/g) of PEF had been reported in in-situ synthesized PEF nanocomposites with multi walled carbon nanotubes or graphene oxide [34]. But it was reported that spherical nanofillers like TiO₂ and SiO₂ nanoparticles did not affect chain growth of PEF in in-situ melt and solid-state polycondensation [29]. To obtain PEF nanocomposites with higher [η], the polycondensation time at 240 °C was prolonged to 2.5 h. Under this condition, it was found that the [η] values of PEF and its nanocomposites increased to 0.71–0.73 dL/g. The effect of DK2 feeding on [η] value of PEF was almost smoothed out. Such results suggest that the gas barrier effect of DK2 on EG removing was not too high and could be overcome to great extent by prolonging the polycondensation time. As a result, PEF nanocomposites with high [η] value were successfully synthesized under suitable conditions.

The ¹H NMR spectrum of PEF shown in Fig. 4 was in accordance with our previous report [25]. The molar percentage of diethylene glycol furandicarboxylate (DEGF) unit formed by etherification side reaction is determined to be 2.31–2.66 mol%. The DEGF content increased slightly with polycondensation time. The ¹H NMR spectra of PEF nanocomposites were almost identical to neat PEF, suggesting that the presence of DK2 did not affect the ¹H NMR measurement. Moreover, the presence of DK2 showed little influence on the formation of DEGF unit, as shown in Table 1.

The presence of hydroxyethyl, a polar reactive group in the organic modifier, should facilitate diffusion of the polar monomers or PEF oligomers into the interlayer of the OMMT. As the main transesterification and polycondensation reactions happened in the bulk, these hydroxyethyl groups could react with the monomers or PEF oligomers that diffused into the interlayer space to generate grafted PEF oligomers or even macromolecular chains. Thus, PEF/MMT with intercalated structure could be formed. With the growth of the grafted or intercalating PEF chains, the interlayer distance of DK2 was expected to grow up and

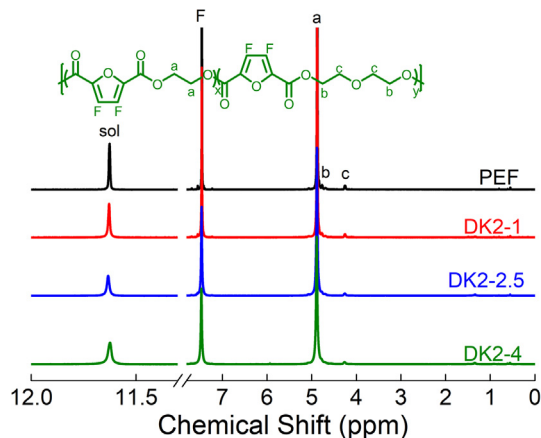


Fig. 4. ¹H NMR spectra of PEF and its nanocomposites. The molar percentage of DEGF repeat unit was calculated with the formula $I_c/(I_a + I_c)$, where I_a and I_c are the integral intensities of chemical shift a and c.

Table 1
Conditions^a and results of the synthesis of PEF and PEF/DK2 nanocomposites.

Run	OMMT (wt%)	t_{mp} (h) ^b	DEGF (mol%) ^c	$[\eta]$ (dl/g) ^d
PEF	0	2	2.31	0.70
		2.5	2.66	0.73
DK2-1	1	2	2.13	0.70
		2.5	2.26	0.71
DK2-2.5	2.5	2	2.39	0.62
		2.5	2.34	0.73
DK2-4	4	2	2.35	0.59
		2.5	2.51	0.72

^a Transesterification conditions: EG:DMFD molar ratio 2:1; 170–200 °C for about 4 h. Polycondensation conditions: 230 °C for 1 h and then 240 °C for t_{mp} indicated in the table.

^b The polycondensation time at 240 °C.

^c Molar percentage of DEGF unit in PEF and its nanocomposites calculated from ¹H NMR shown in Fig. 4.

^d Intrinsic viscosity measured at 25 °C using the mixture of phenol/1,1,2,2-tetrachloroethane (3/2, w/w).

finally, PEF/MMT nanocomposites with exfoliated or at least partially exfoliated structure could be obtained. The synthetic principle is sketched in Scheme 1.

As shown in Fig. 3, DK2 shows the characteristic diffraction peak at 3.32°, corresponding to an interlayer distance d_{001} of 2.42 nm. But no characteristic diffraction peak of DK2 was observed in the three PEF nanocomposites, suggesting the exfoliated structure or at minimum destructure/delamination of the starting organically modified clay layer stacks. It can be observed from the TEM micrographs shown in Fig. 5 that indeed exfoliation advantageously takes place but only partially since it remains some disordered intercalated stacks in the PEF nanocomposites.

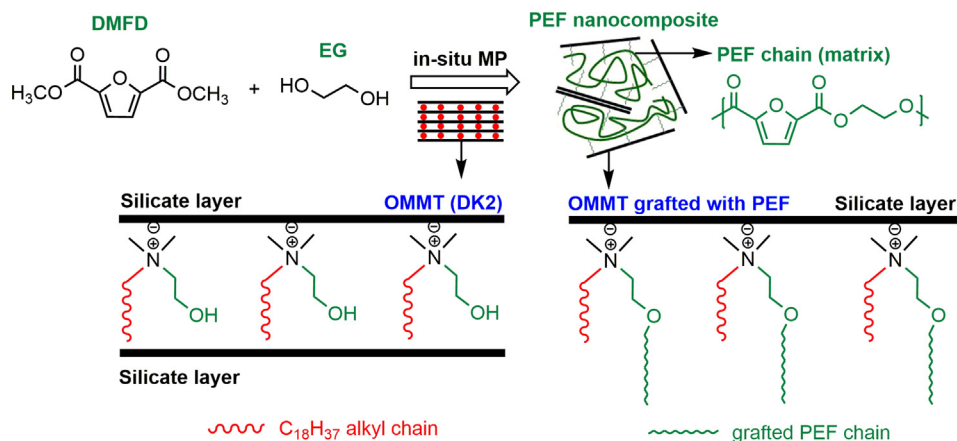
To verify the hypothesis that some PEF chains were grafted from the surface of OMMT, the PEF-grafted OMMT was isolated and characterized with FTIR. The nanocomposite DK2-2.5 was dissolved in a solvent mixture composed of phenol and TCE. The resulting dispersion was treated by multiple cycles of high-speed centrifugation and washing until no polymer in the supernatant could be detected by precipitation with excessive ethanol. The so-recovered sample was coined as DK2-2.5g. The sample was dried at 70 °C under vacuum and then used for FTIR characterization. For comparison, 2.5 wt% (based on PEF) DK2 was directly dispersed in PEF solution. The same centrifugation/washing treatment was performed and the resulting sample identified as DK2-2.5 m was also characterized with FTIR. From Fig. 1, it is clear that the FTIR spectrum of DK2-2.5g resembles well to that of the nanocomposite DK2-2.5. Strong characteristic absorptions of PEF, namely, stretching vibration of CH in the furan ring at 3126 cm^{-1} , stretching

vibration of C = O and C-O in the ester bonds at 1713 cm^{-1} and 1263 cm^{-1} respectively are observed in both DK2-2.5 and DK2-2.5g. However, the feature absorptions of DK2 are very weak or overlapped. In contrast, the sample DK2-2.5 m showed strong characteristic absorptions of DK2 at 3621 cm^{-1} , 2919 cm^{-1} , 2850 cm^{-1} and 1030 cm^{-1} , but the peaks attributed to PEF are much weaker than DK2-2.5g. Therefore, it can be concluded that PEF chains have been successfully grafted onto the surface of OMMT due to the transesterification reaction between the monomers and/or PEF oligomers together with the reactive organic modifiers, i.e., hydroxy groups of the octadecyl hydroxyethyl dimethyl ammonium cations covering the surface of the negatively charged clay platelets.

3.2. Thermal transition behavior

The DSC thermograms of PEF and its nanocomposites are shown in Fig. 6 and the thermal transition properties are summarized in Table 2. The PEF sample exhibited glass transition temperature (T_g) as high as 91 °C and a weak melting peak (~ 2.5 J/g) at about 211 °C in the second heating scans, but showed neither melt nor cold crystallization during cooling and second heating scans. In fact, it has been extensively reported that PEF is a crystallizable polyester, but its crystallization rate is usually slow, especially from melt. Therefore and as pointed out in the Introduction section, promoting PEF crystallization is very desirable from the viewpoint of PEF modification. Previous studies indicated that the presence of 2.5 wt% MWCNT and GO nanofillers clearly promoted melt crystallization of PEF at cooling rate of 5 °C/min [34], but so far the crystallization of PEF proved to be slightly promoted by OMMT (as tentatively dispersed by conventional blending) even at a slow cooling rate of 2 °C/min. [30]

For the three nanocomposites with intrinsic viscosity (0.71–0.73 dL/g) comparable to the pristine PEF, the crystallization behavior strongly depended on the OMMT loading. For DK2-1, only cold crystallization with an enthalpy of 10 J/g around 175 °C was observed in the 2nd heating. Interestingly enough, both melt crystallization (9.9 J/g, 150 °C) and cold crystallization (12.1 J/g, 167 °C) appeared for DK2-2.5. However, DK2-4 did not crystallize during cooling and second heating at 10 °C/min though a weak (but still stronger than PEF) melting peak was observed in the first heating. Such a result implies that agglomeration of OMMT might occur in DK2-4. What is interesting is that the DK2-2.5 sample with lower $[\eta]$ (0.62 dL/g) showed much faster melt crystallization (27.4 J/g) at higher temperature (156 °C). Therefore, the crystallization of PEF nanocomposite also depends on the molecular weight (MW) of PEF matrix. In fact, strong MW dependence of PEF crystallization rate has been reported by van Berkel *et al.* [43] and also found in our previous research [13]. In conclusion, the in-situ



Scheme 1. Schematic representation of synthesis of PEF/MMT nanocomposites via in-situ polycondensation of DMFD and EG in the presence of OMMT (DK2) modified with octadecyl hydroxyethyl dimethyl ammonium, along with PEF chain grafting from the silicate layers.

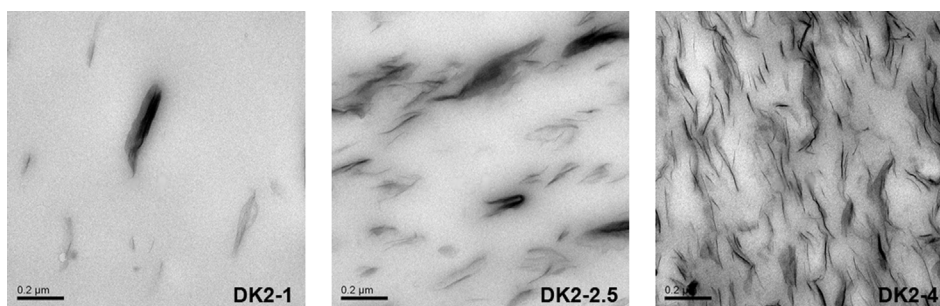


Fig. 5. TEM micrographs of in-situ synthesized PEF/MMT nanocomposites containing various amounts of DK2. (from left to right: DK2-1, DK2-2.5, DK2-4).

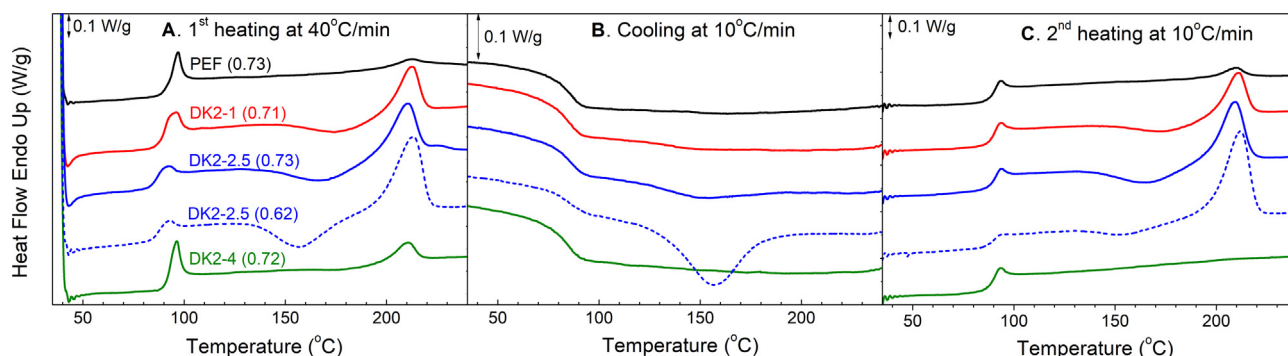


Fig. 6. DSC thermograms of PEF and its nanocomposites: A. First heating scan at 40 °C/min; B. Cooling scan at 10 °C/min; C. Second heating scan at 10 °C/min. Note: The data in the parenthesis after the sample name indicates the intrinsic viscosity in the unit of dL/g of the sample.

Table 2

Thermal properties of PEF and its nanocomposites.

Sample ^a	Cooling scan		First/second heating scan					TGA ^b	
	T_c (°C)	ΔH_c (J·g ⁻¹)	T_g (°C)	T_{cc} (°C)	ΔH_{cc} (J·g ⁻¹)	T_m (°C)	ΔH_m (J·g ⁻¹)	$T_{d,5}$ (°C)	T_{max} (°C)
PEF (0.73)	nd	nd	92/91	nd/nd	nd/nd	212/211	2.7/2.5	351	375
DK2-1 (0.71)	146	2.1	90/91	176/175	11.6/10.0	213/211	12.5/12.0	354	378
DK2-2.5 (0.73)	150	9.9	89/91	171/167	16.2/12.1	210/209	17.1/21.6	353	381
DK2-2.5 (0.62)	156	27.3	89/91	158/154	20.1/6.0	213/212	30.7/33.8	–	–
DK2-4 (0.72)	nd	nd	91/91	177/nd	2/nd	210/210	5.6/1.0	351	378

^a The data in the parenthesis after the sample name indicates the intrinsic viscosity (dL/g) of the sample.

^b Decomposition temperature at 5% ($T_{d,5}$) and maximum decomposition rate (T_{max}) measured with TGA at 10 °C/min under N₂ atmosphere.

synthesized PEF/DK2 nanocomposite containing 2.5 wt% DK2 manifests greatly improved crystallization with respect to pristine PEF.

3.3. Crystal structure

The crystal structure of PEF and DK2-2.5 were investigated by X-ray diffraction. Prior to testing, both PEF and DK2-2.5 were melted, quenched and at last isothermally cold crystallized at 150 °C and 190 °C for 3 h, respectively. The result was shown in Fig. 7. According to previous reports [44–46], as for PEF, the stable triclinic α -PEF crystalline phase, the less stable monoclinic α' -PEF crystalline phase and the monoclinic β -PEF crystalline phase can be formed under high-crystallization temperature ($T_c > 170$ °C), low-crystallization temperature ($T_c < 170$ °C) and solvent-induced crystallization treatment, respectively. In this work, as expected for PEF, typical α' (2θ 16.2°, 18.0°, 20.5°, 23.4°, 26.5°) and α (2θ 16.3°, 18.1°, 19.5°, 20.8°, 23.6°, 26.8°) crystalline phases were formed upon cold crystallization at 150 °C and 190 °C, respectively. However, the DK2-2.5 sample showed the same α' crystalline phase, being independent of the cold crystallization temperature, 150 °C and 190 °C. The result suggests that it is prone for the nanocomposite to form the α' crystalline phase even at high cold crystallization temperature (190 °C). Similar result has also

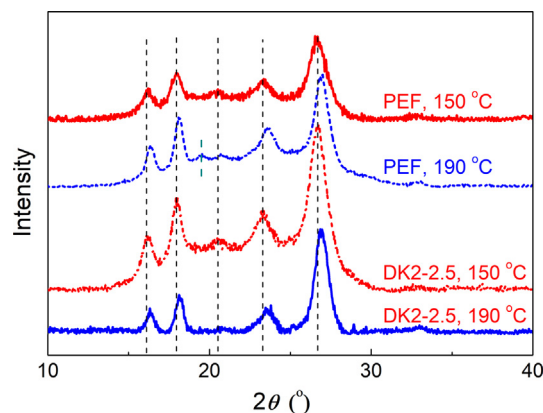


Fig. 7. WAXD patterns of PEF and DK2-2.5 isothermally cold crystallized at the indicated temperature after quenched from melt.

been reported by Iotti *et al.* [34]. The α' -PEF crystalline phase was found in the second heating process (over 175 °C) of PEF-MWCNTs nanocomposite after melt quenching. [34]

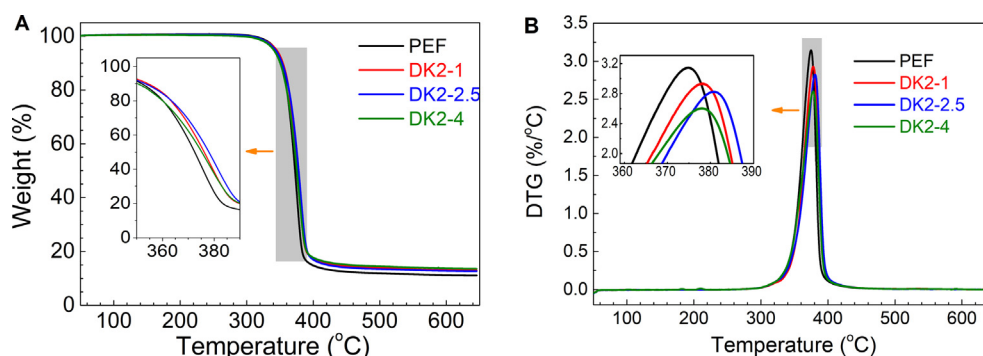


Fig. 8. TGA (A) and DTG (B) curves of PEF and PEF/MMT nanocomposites under N_2 atmosphere at heating rate of $10^\circ C/min$.

Table 3

Tensile properties of PEF and PEF/DK2 nanocomposites

Sample	$[\eta]$ (dl/g)	E (GPa)	σ_b (MPa)	ϵ_b (%)
PEF	0.73	3.4 ± 0.5	85 ± 2	2.9 ± 0.9
DK2-1	0.71	3.7 ± 0.4	103 ± 5	3.8 ± 1.6
DK2-2.5	0.73	4.1 ± 0.1	113 ± 5	3.9 ± 0.8
DK2-4	0.72	4.6 ± 0.3	84 ± 9	1.6 ± 0.4

Note: the stretching rate used was 1 mm/min.

3.4. Thermal stability

PEF and its nanocomposites manifested satisfactory thermal stability, as shown in Fig. 8 and Table 2. They did not show discernable decomposition before $300^\circ C$. It is clear that the nanocomposite DK-1 and DK2-2.5 showed a highest $T_{d,5}$ and T_{max} of $354^\circ C$ and $381^\circ C$, respectively, being ca. $3^\circ C$ and $6^\circ C$ higher than that of PEF. Such improvement may be related to the barrier effect of OMMT on diffusion and volatilization of gas products formed by thermal decomposition. But the difference is so small that it can be concluded that the PEF nanocomposites showed almost the same thermal stability with respect to pristine PEF. In other words, the presence of DK2 did not clearly affect the thermal decomposition of PEF matrix. Thermal stability of polymer nanocomposites depends on nanofiller nature, exfoliation/dispersion state and organic-inorganic interaction. Unchanged thermal stability was also observed in other polyester/DK2 nanocomposites at similar DK2 loading range [47] and in PEF/ TiO_2 and PEF/ SiO_2 nanocomposites [29]. But improvement in thermal stability was also reported for PEF/MMT nanocomposites prepared with both solvent [30] and melt blending [32]. Differently, PEF/MWCNT-COOH and PEF/GO nanocomposites showed deteriorated thermal stability with respect to neat PEF [34].

3.5. Mechanical properties

The tensile properties of PEF and its nanocomposites are summarized in Table 3. The pristine PEF showed tensile properties comparable to those of the PEFs synthesized with Ti-based catalyst in our previous reports [8,24,25]. The nanocomposites manifested similar brittle fracture behavior but superior tensile modulus and strength. The Young's modulus (E) increased continuously with increasing DK2 loading, from 3.4 GPa of PEF to 4.6 GPa of DK2-4. The stress at break (σ_b) also increased with DK2 loading, reaching the maximum 113 MPa at 2.5 wt% DK2. But at higher DK2 loading of 4 wt%, the σ_b value decreased to be comparable to that of PEF. The elongation at break (ϵ_b) showed similar DK2 loading dependence with σ_b . But the variation in ϵ_b was very small, being within the margin of measurement error.

Among the three nanocomposites, DK2-2.5 possesses the best tensile properties. With respect to pristine PEF, its modulus and strength increased by 20% and 33% respectively. The significant improvements in

Young's modulus and tensile strength are attributed to the exfoliation, at least partially, and fine dispersion of montmorillonite nanoparticles, the interaction between PEF matrix and the nanoparticles arising from the above mentioned PEF chain grafting and promoted crystallization. At higher DK2 loading like 4 wt%, partial nanoparticles agglomerated and the crystallization promotion effect disappeared, leading to the decreased tensile strength. To the best of our knowledge, this is the first report on mechanical properties of PEF nanocomposites.

4. Conclusions

Biobased PEF/MMT nanocomposites with PEF intrinsic viscosity over 0.70 dL/g and partially exfoliated structure were in-situ synthesized via melt polycondensation of DMFD and EG in the presence of a commercially available organic modified montmorillonite, DK2. It was found that PEF chain grafting from the surface of MMT occurred along with the transesterification/polycondensation reaction in the bulk. The presence of the grafted PEF chains contributed to partial exfoliation of OMMT and the interaction between MMT and PEF matrix. With respect to pristine PEF, the PEF nanocomposites containing 2.5 wt% DK2 showed significantly improved melt crystallization (up to 27.3 J/g), tensile modulus (4.1 GPa) and strength (113 MPa). In the presence of DK2, it is prone for the nanocomposite to form the α' -PEF crystalline phase, even at cold crystallization temperature higher than $170^\circ C$.

Declaration of Competing Interest

The authors declare that they have no known competing financial interests or personal relationships that could have appeared to influence the work reported in this paper.

Acknowledgements

This work was supported by the National Natural Science Foundation of China (51773177), State Key Laboratory of Chemical Engineering (No. SKL-ChE-18D02) and 151 Talents Project of Zhejiang Province. The authors thank Dr. Jijiang Hu, Ms Qun Pu, Ms Li Xu for their assistance in specimen processing, characterization and testing at State Key Laboratory of Chemical Engineering (Zhejiang University).

Data availability

The raw/processed data required to reproduce these findings cannot be shared at this time due to technical or time limitations. Data will be made available upon request.

References

- J.J. Bozell, G.R. Petersen, Technology development for the production of biobased products from biorefinery carbohydrates—the US department of energy's "Top 10" revisited, *Green Chem.* 12 (2010) 539–551.

- [2] A. Boisen, T.B. Christensen, W. Fub, Y.Y. Gorbanev, T.S. Hansenv, J.S. Jensen, S.K. Klitgaard, S. Pedersen, A. Riisager, T. Stahlberg, J.M. Woodley, Process integration for the conversion of glucose to 2,5-furandicarboxylic acid, *Chem. Eng. Res. Des.* 87 (2009) 1318–1327.
- [3] B. Pereira, H. Zhang, M.M. De, C.G. Lim, Z.J. Li, G. Stephanopoulos, Engineering a novel biosynthetic pathway in *Escherichia coli* for production of renewable ethylene glycol, *Biotechnol. Bioeng.* 113 (2016) 376–383.
- [4] H. Liu, K.R.M. Ramos, K.N.G. Valdehuesa, G.M. Nisola, W.K. Lee, W.J. Chung, Biosynthesis of ethylene glycol in *Escherichia coli*, *Appl. Microbiol. Biot.* 97 (2013) 3409–3417.
- [5] A.J.J.E. Eerhart, A.P.C. Faaij, M.K. Patel, Replacing fossil based PET with biobased PEF; process analysis, energy and GHG balance, *Energ. Environ. Sci.* 5 (4) (2012) 6407–6422.
- [6] G.Z. Papageorgiou, V. Tsanakis, D.N. Bikiaris, Synthesis of poly(ethylene furandicarboxylate) polyester using monomers derived from renewable resources: thermal behavior comparison with PET and PEN, *PCCP* 16 (2014) 7946–7958.
- [7] G.Z. Papageorgiou, D.G. Papageorgiou, Z. Terzopoulou, D.N. Bikiaris, Production of bio-based 2,5-furan dicarboxylate polyesters: recent progress and critical aspects in their synthesis and thermal properties, *Eur. Polym. J.* 83 (2016) 202–229.
- [8] H.Z. Xie, L.B. Wu, B.G. Li, P. Dubois, Modification of poly(ethylene 2,5-furandicarboxylate) with biobased 1,5-pentanediol: Significantly toughened copolymers retaining high tensile strength and O₂ barrier property, *Biomacromolecules* 20 (2019) 353–364.
- [9] J.G. Wang, X.Q. Liu, Y.J. Zhang, F. Liu, J. Zhu, Modification of poly(ethylene 2,5-furandicarboxylate) with 1,4-cyclohexanedimethylene: influence of composition on mechanical and barrier properties, *Polymer* 103 (2016) 1–8.
- [10] S.K. Burgess, O. Karvan, J.R. Johnson, R.M. Kriegel, W.J. Koros, Oxygen sorption and transport in amorphous poly(ethylene furanoate), *Polymer* 55 (18) (2014) 4748–4756.
- [11] S.K. Burgess, R.M. Kriegel, W.J. Koros, Carbon dioxide sorption and transport in amorphous poly(ethylene furanoate), *Macromolecules* 55 (18) (2015) 4748–4756.
- [12] G.Z. Papageorgiou, T. Vasilios, D.N. Bikiaris, Synthesis of poly(ethylene furandicarboxylate) polyester using monomers derived from renewable resources: thermal behavior comparison with PET and PEN, *PCCP* 16 (17) (2014) 7946–7958.
- [13] J.P. Wu, H.Z. Xie, L.B. Wu, P. Dubois, DBU-catalyzed biobased poly(ethylene 2,5-furandicarboxylate) polyester with rapid melt crystallization: synthesis, crystallization kinetics and melting behavior, *RSC Adv.* 6 (103) (2016) 101578–101586.
- [14] A. Codou, N. Guigo, J.G. van Berkel, E.D. Jong, N. Sbirrazzuoli, Non-isothermal crystallization kinetics of biobased poly(ethylene 2,5-furandicarboxylate) synthesized via the direct esterification process, *Macromol. Chem. Phys.* 215 (21) (2014) 2065–2074.
- [15] M. Jiang, Q. Liu, Q. Zhang, C. Ye, G.Y. Zhou, A series of furan-aromatic polyesters synthesized via direct esterification method based on renewable resources, *J. Polym. Sci. Part A Polym. Chem.* 50 (5) (2012) 1026–1036.
- [16] R.J.I. Knoop, W. Vogelzang, J.V. Haveren, Es DSV. High molecular weight poly(ethylene-2,5-furanoate); critical aspects in synthesis and mechanical property determination, *J. Polym. Sci. Part A Polym. Chem.* 51 (19) (2013) 4191–4199.
- [17] G.Q. Wang, M. Jiang, Q. Zhang, R. Wang, G.Y. Zhou, Biobased copolymers: synthesis, crystallization behavior, thermal and mechanical properties of poly(ethylene glycol sebacate-co-ethylene glycol 2,5-furandicarboxylate), *RSC Adv.* 7 (23) (2017) 13798–13807.
- [18] S. Hong, O.O. Park, High molecular weight bio furan-based co-polyesters for food packaging applications, *Green Chem.* 18 (19) (2016) 5142–5150.
- [19] G.Q. Wang, M. Jiang, Q. Zhang, R. Wang, G.Y. Zhou, Biobased multiblock copolymers: synthesis, properties and shape memory performance of poly(ethylene-2,5-furandicarboxylate)-b-poly(ethylene glycol), *Polym. Degrad. Stab.* 144 (2017) 121–127.
- [20] J.G. Wang, X.Q. Liu, Z. Jia, Y. Liu, L.Y. Sun, J. Zhu, Synthesis of bio-based poly(ethylene 2,5-furandicarboxylate) copolymers: higher glass transition temperature, better transparency, and good barrier properties, *J. Polym. Sci. Part A Polym. Chem.* 55 (2017) 3298–3307.
- [21] J.G. Wang, X.Q. Liu, Z. Jia, L.Y. Sun, Y.J. Zhang, J. Zhu, Modification of poly(ethylene 2,5-furandicarboxylate) (PEF) with 1,4-cyclohexanedimethanol: Influence of stereochemistry of 1,4-cyclohexylene units, *Polymer* 137 (2018) 173–185.
- [22] X.S. Wang, S.Y. Liu, Q.Y. Wang, J.G. Li, G.Y. Wang, Synthesis and characterization of poly(ethylene 2,5-furandicarboxylate-co-ε-caprolactone) copolymers, *Euro. Polym. J.* 109 (2018) 191–197.
- [23] X.S. Wang, Q.Y. Wang, S.Y. Liu, G.Y. Wang, Biobased copolymers: Synthesis, structure, thermal and mechanical properties of poly(ethylene 2,5-furandicarboxylate-co-ethylene 1,4-cyclohexanedicarboxylate), *Polym. Degrad. Stab.* 154 (2018) 96–102.
- [24] H.Z. Xie, L.B. Wu, B.G. Li, P. Dubois, Biobased poly(ethylene-co-hexamethylene 2,5-furandicarboxylate) (PEHF) copolymers with superior tensile properties, *Ind. Eng. Chem. Res.* 57 (2018) 13094–13102.
- [25] H.Z. Xie, L.B. Wu, B.G. Li, P. Dubois, Poly(ethylene 2,5-furandicarboxylate-*mb*-poly(tetramethylene glycol)) multiblock copolymers: from high tough thermoplastics to elastomers, *Polymer* 155 (2018) 89–98.
- [26] Y. Chen, M. Jiang, C.J. Sun, Q. Zhang, Z.P. Fu, L. Xu, G.Y. Zhou, Preparation and characterization of poly(ethylene 2,5-furandicarboxylate)/poly(butylene succinate) blends, *Chin. J. Appl. Chem.* 32 (2015) 1022–1027.
- [27] N. Pouloupoulou, N. Kasmi, D.N. Bikiaris, D.G. Papageorgiou, G. Floudas, G.Z. Papageorgiou, Sustainable polymers from renewable resources: polymer blends of furan-based polyesters, *Macromol. Mater. Eng.* 303 (2018) 1800153.
- [28] N. Pouloupoulou, N. Kasmi, M. Siampani, Z.N. Terzopoulou, D.N. Bikiaris, D.S. Achilias, D.G. Papageorgiou, G.Z. Papageorgiou, Exploring next-generation engineering bioplastics: poly(alkylene furanoate)/poly(alkylene terephthalate) (PAF/PAT) blend, *Polymers* 11 (2019) 556.
- [29] D.S. Achilias, A. Chondroyannis, M. Nerantzaki, K.V. Adam, Z. Terzopoulou, G.Z. Papageorgiou, D.N. Bikiaris, Solid state polymerization of poly(ethylene furanoate) and its nanocomposites with SiO₂ and TiO₂, *Macromol. Mater. Eng.* 302 (7) (2017) 1700012.
- [30] L. Martino, V. Niknam, N. Guigo, J.G. van Berkel, N. Sbirrazzuoli, Morphology and thermal properties of novel clay-based poly(ethylene 2,5-furandicarboxylate) (PEF) nanocomposites, *RSC Adv.* 6 (2016) 59800.
- [31] A. Codou, N. Guigo, J.G. van Berkel, E.D. Jong, N. Sbirrazzuoli, Preparation and characterization of poly(ethylene 2,5-furandicarboxylate)/nanocrystalline cellulose composites via solvent casting, *J. Polym. Eng.* 37 (9) (2017) 869–878.
- [32] L. Martino, N. Guigo, J.G. van Berkel, N. Sbirrazzuoli, Influence of organically modified montmorillonite and sepiolite clay on the physical properties of bio-based poly(ethylene 2,5-furandicarboxylate), *Compos. Part B Eng.* 110 (2017) 96–105.
- [33] A. Codou, N. Guigo, J.G. van Berkel, J.E. De, N. Sbirrazzuoli, Preparation and crystallization behavior of poly(ethylene 2,5-furandicarboxylate)/cellulose composites by twin screw extrusion, *Carbohydr. Polym.* 174 (2017) 1026–1033.
- [34] N. Lotti, A. Munari, M. Gigli, M. Gazzano, V. Tsanakis, D.N. Bikiaris, G.Z. Papageorgiou, Thermal and structural response of in situ prepared biobased poly(ethylene 2,5-furan dicarboxylate) nanocomposites, *Polymer* 103 (2016) 288–298.
- [35] M.B. Nasirudeen, H.C. Hailes, J.R.G. Evans, Preparation and characterization of biobased poly(ethylene 2,5-furandicarboxylate)/clay nanocomposites, *Niger. J. Bas. Appl. Sci.* 25 (2) (2017) 114–124.
- [36] M.A. Ortenzi, L. Basilissi, H. Farina, G.D. Silvestro, L. Piergiovanni, E. Mascheroni, Evaluation of crystallinity and gas barrier properties of films obtained from PLA nanocomposites synthesized via “in situ” polymerization of L-lactide with silane-modified nanosilica and montmorillonite, *Eur. Polym. J.* 66 (2015) 478–491.
- [37] T. Wan, L. Chen, Y.C. Chua, X.H. Lu, Crystallization morphology and isothermal crystallization kinetics of poly(ethylene terephthalate)/clay nanocomposites, *J. Appl. Polym. Sci.* 94 (2004) 1381–1388.
- [38] A. Dorigato, M. Sebastiani, A. Pegoretti, L. Fambri, Effect of silica nanoparticles on the mechanical performances of poly(lactic acid), *J. Polym. Environ.* 20 (2012) 713–725.
- [39] M. Yourdkhani, T. Mousavand, N. Chapleau, P. Hubert, Thermal, oxygen barrier and mechanical properties of polylactide-organoclay nanocomposites, *Compos. Sci. Technol.* 82 (2013) 47–53.
- [40] A. Mirzadeh, M. Kokabi, The effect of composition and draw-down ratio on morphology and oxygen permeability of polypropylene nanocomposite blown films, *Eur. Polym. J.* 43 (2007) 3757–3765.
- [41] Y. Lin, H.B. Chen, C.M. Chan, J.S. Wu, The toughening mechanism of polypropylene/calcium carbonate nanocomposites, *Polymer* 51 (2010) 3277–3284.
- [42] H. Balakrishnan, A. Hassan, M. Imran, M.U. Wahit, Toughening of polylactic acid nanocomposites: a short review, *Polym. Plast. Technol.* 51 (2012) 175–192.
- [43] J.G. van Berkel, N. Guigo, J.J. Kolstad, L. Sipos, B. Wang, M.A. Dam, N. Sbirrazzuoli, Isothermal crystallization kinetics of poly(ethylene 2,5-furandicarboxylate): isothermal crystallization kinetics of poly(ethylene 2,5-furandicarboxylate), *Macromol. Mater. Eng.* 300 (4) (2015) 466–474.
- [44] G. Stoclet, G.G. du Sart, B. Yeniad, S. de Vos, J.M. Lefebvre, Isotherma crystallization and structural characterization of poly(ethylene-2,5-furanoate), *Polymer* 72 (2015) 165–175.
- [45] V. Tsanakis, D.G. Papageorgiou, S. Exarhopoulos, D.N. Bikiaris, G.Z. Papageorgiou, Crystallization and polymorphism of poly(ethylene furanoate), *Cryst. Growth Des.* 15 (2015) 5505–5512.
- [46] L. Maini, M. Gigli, M. Gazzano, N. Lotti, D.N. Bikiaris, G.Z. Papageorgiou, Structural investigation of poly(ethylene furanoate) polymorphs, *Polymers* 10 (2018) 296.
- [47] J.X. Li, L. Lai, L.B. Wu, S.J. Severtson, W.J. Wang, Enhancement of water vapor barrier properties of biodegradable poly(butylene adipate-co-terephthalate) films with highly oriented organomontmorillonite, *ACS Sustain. Chem. Eng.* 6 (2018) 6654–6662.